

Fingerprints of High-Dimensional Coexistence in Complex Ecosystems

Matthieu Barbier

*Centre for Biodiversity Theory and Modelling, Theoretical and Experimental Ecology Station,
CNRS and Paul Sabatier University, 09200 Moulis, France
and Institut Natura e Teoria en Pireneus, 75015 Paris, France*

Claire de Mazancourt and Michel Loreau

*Centre for Biodiversity Theory and Modelling, Theoretical and Experimental Ecology Station,
CNRS and Paul Sabatier University, 09200 Moulis, France*

Guy Bunin 

Department of Physics, Technion-Israel Institute of Technology, Haifa 3200003, Israel



(Received 4 August 2020; revised 27 October 2020; accepted 2 December 2020; published 14 January 2021)

The coexistence of many competing species in an ecological community is a long-standing theoretical and empirical puzzle. Classic approaches in ecology assume that species fitness and interactions in a given environment are mainly driven by a few essential species traits, and coexistence can be explained by trade-offs between these traits. The apparent diversity of species is then summarized by their positions (“ecological niches”) in a low-dimensional trait space. Yet, in a complex community, any particular set of traits and trade-offs is unlikely to encompass the full organization of the community. A diametrically opposite approach assumes that species interactions are disordered, i.e., essentially random, as might arise when many species traits combine in complex ways. This approach is appealing theoretically, and can lead to novel emergent phenomena, fundamentally different from the picture painted by low-dimensional theories. Nonetheless, fully disordered interactions are incompatible with many-species coexistence, and neither disorder nor its dynamical consequences have received direct empirical support so far. Here we ask what happens when random species interactions are minimally constrained by coexistence. We show theoretically that this leads to testable predictions. Species interactions remain highly disordered, yet with a “diffuse” statistical structure: interaction strengths are biased so that successful competitors subtly favor each other, and correlated so that competitors partition their impacts on other species. We provide strong empirical evidence for this pattern, in data from grassland biodiversity experiments that match our predictions quantitatively. This is a first-of-a-kind test of disorder on empirically measured interactions, and unique evidence that species interactions and coexistence emerge from an underlying high-dimensional space of ecological traits. Our findings provide a new null model for inferring interaction networks with minimal prior information and a set of empirical fingerprints that support a statistical physics-inspired approach of complex ecosystems.

DOI: [10.1103/PhysRevX.11.011009](https://doi.org/10.1103/PhysRevX.11.011009)

Subject Areas: Biological Physics,
Statistical Physics

I. INTRODUCTION

While species-rich ecosystems are often too complex for an exhaustive description, we can strive to understand them from two complementary approaches. The first is to identify the role of particular species, traits, and environmental factors. The second approach is to search for

collective phenomena that cannot be ascribed to any individual species, but emerge from their interplay.

The contrast between these approaches is clearly manifest in the problem of coexistence. Coexistence is a long-standing puzzle in ecology: various theories and experiments have brought forward the principle of competitive exclusion, whereby the best competitor should displace all others [1,2]. Yet, strict dominance by one species appears to be the exception rather than the rule in the natural world, and many communities host a remarkable diversity of competitors [3].

Following the first approach, this puzzle is tackled by positing *coexistence mechanisms* that may allow species to

Published by the American Physical Society under the terms of the Creative Commons Attribution 4.0 International license. Further distribution of this work must maintain attribution to the author(s) and the published article's title, journal citation, and DOI.

coexist, through particular trade-offs between species traits, such as exploitation [4], defense against predators [5], and tolerance to environmental fluctuations [6,7]. Such coexistence mechanisms are low dimensional, in that meaningful differences between species are reduced to their positions along one or a handful of specific dimensions (a few essential traits). Trade-offs translate to constraints on species interactions, on their strength, and their arrangement [8]. For instance, the competition-colonization trade-off [9,10] posits a strict hierarchy in the competitive ability of species, from weakest to strongest, precisely counterbalanced by their growth ability. If we increase the number of species that must coexist, these constraints become more and more restrictive and select a smaller and smaller subset of all interaction networks that might exist.

A radically different approach argues that if the ecosystem is complex, with many interaction mechanisms at play, a better starting point is to assume that many of the system's details can be replaced with some form of randomness [11]; see Fig. 1. This is a bold move, yet one that parallels major successes in physics and other fields [12–15]. The large body of theoretical work building on this assumption predicts that high dimensionality will lead to collective, emergent phenomena such as phase transitions, driven by

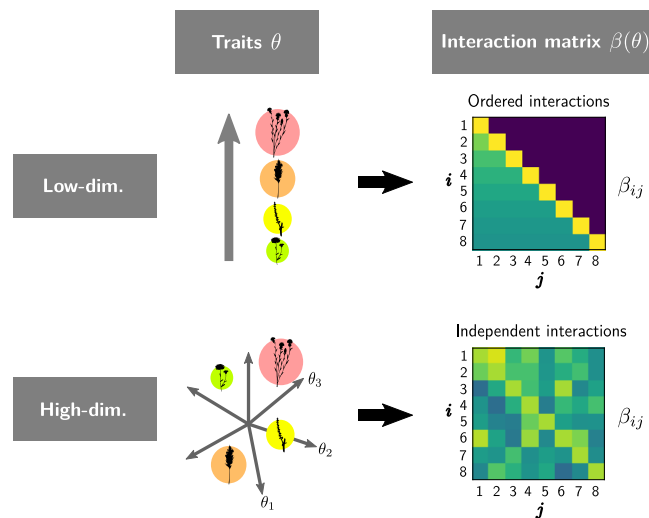


FIG. 1. Dimensionality of interaction patterns. The network of pairwise interactions between S species can be represented by a $S \times S$ matrix (square box) where each element β_{ij} denotes the effect of species j on η_i , the relative yield of species i defined in Eq. (1). We assume that interactions β are constant in time, and entirely determined by underlying species traits and limiting factors θ , for instance representing resources, pathogens, or behaviors. In a low-dimensional trait space, each species is characterized by a few traits; therefore the interaction matrix can be ordered by trait values and displays a simple organization. In a high-dimensional trait space, each interaction is a complex combination of factors, potentially unique and independent of other interactions. This can lead to a matrix without conspicuous order, often modeled as a random matrix [11–14].

a small number of statistics of the interaction network [11,16–23]. This is very different from the picture arising from low-dimensional coexistence mechanisms. Randomness is also often used, either explicitly or implicitly, to make up for the poverty of data, when compared with possibly thousands of parameters required to fully reconstruct the dynamical rules in large ecosystems.

Despite its rich promise, the latter approach has so far received limited theoretical development and empirical support, and it is not clear when and how the two approaches apply. Collective phenomena that follow from high dimensionality have yet to be empirically demonstrated. Demonstrating high dimensionality via direct examination of the interactions is also hard: Ideally, one would directly measure the type and strength of each interaction, and look for signs of high dimensionality there. This is difficult, firstly since it is generally hard to correctly infer interaction strength, and when possible, prone to large measurement errors. It is then not clear what one should test when looking for “randomness,” especially when inferred interactions are noisy. Another challenge comes from the constraints that coexistence imposes on the possible set of species interactions, that must somehow be incorporated into the theory, in a role analogous to low-dimensional coexistence mechanisms.

Here we ask what happens when random pairwise interactions are minimally constrained to allow species to coexist. Even though very little is assumed, the theory makes precise testable predictions that are far from obvious. While these predictions follow from the assumption of randomlike interactions, they involve self-averaging quantities that are less sensitive to measurement errors, allowing to check them against empirical data. We test these predictions and show that they quantitatively hold in detail, in data from long-running plant biodiversity experiments.

We predict that species coexistence can be achieved without any conspicuous order in the ecological network. Coexistence requires only a subtle statistical structure (referred to below as a *pattern*), where “diffuse” changes in means and correlations throughout the network bias how the most successful competitors interact with other species. We uncover this latent structure by an inferential approach shown in Fig. 2. We ask, if one samples many different interaction networks, and retains only those in which all species survive, what do the remaining networks have in common? Some may appear very structured, others almost random. Yet, we find that *most* of these networks exhibit the same statistical pattern, expressed in equations below. We derive this pattern from a simple probabilistic argument, explain in intuitive terms how it allows coexistence, and validate this pattern quantitatively in interaction networks inferred from biodiversity experiments. We then discuss how this pattern may arise from species selection and how it relates to dynamical properties of the ecosystem.

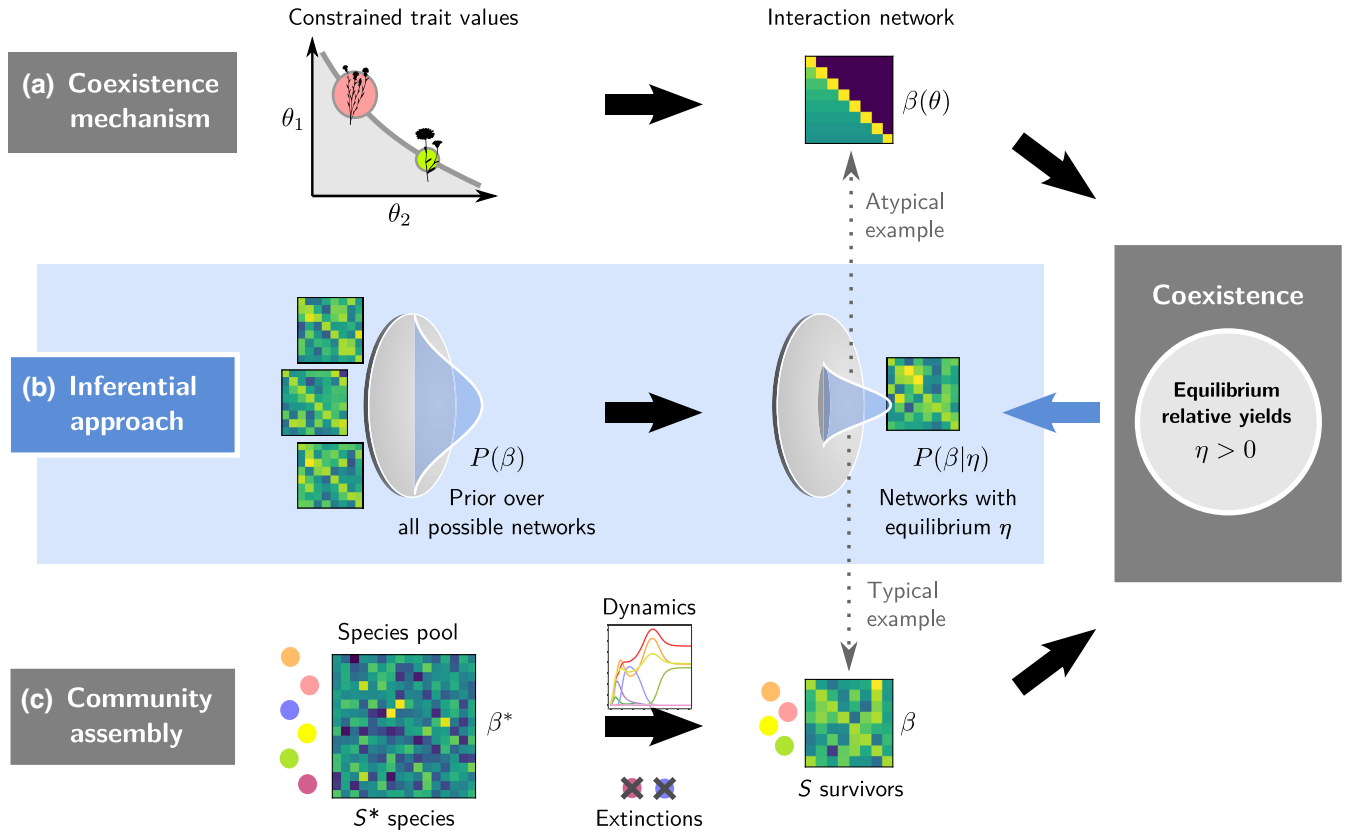


FIG. 2. Three approaches to coexistence. (a) An equilibrium coexistence mechanism can be expressed as a specific pattern in the network of species interactions. To allow coexistence, i.e., an equilibrium where all species have positive relative yields η as defined in Eq. (1), the traits θ which determine species interactions $\beta(\theta)$ must follow particular relations or constraints. We show here the classic low-dimensional example of a trade-off between two traits (competitive ability and colonization rate [9,10]; see Supplemental Material [24]). (b) Our inferential approach reverses the direction of reasoning: given that we observe species coexisting at equilibrium in nature, we can infer the most likely distribution of interactions that could have caused this equilibrium, i.e., the posterior distribution $P(\beta|\bar{\eta})$ given a prior $P(\beta)$ over all possible interaction networks. If we choose a high-dimensional prior (independent interactions), communities drawn from the posterior distribution retain random-looking but correlated interactions, with simple and predictable statistical features: a “diffuse clique” pattern described below. (c) Community assembly (see Sec. III) involves a larger pool of $S_{\text{pool}} > S$ species, here with independent interactions. Through ecological dynamics, some of these species go extinct or cannot invade, leading to a smaller persistent group of S species whose interactions β have been dynamically selected to allow coexistence. Dotted arrows: The assembled community in (c) precisely follows the statistical properties of communities drawn from the posterior distribution in (b), if we assume independent interactions for both the inference prior and pool distribution [25]. Low-dimensional structures, such as illustrated here in (a), can be seen as possible but very improbable matrices in this distribution, and can exhibit different patterns from our diffuse clique prediction. We can interpret the posterior distribution $P(\beta|\bar{\eta})$ as a null model for coexistence in the presence of many biological mechanisms. The resulting diffuse clique pattern represents a form of collective organization, where coexistence arises, not from particular species traits, but from statistical biases distributed over all interactions.

II. RESULTS

A. Theoretical setting

We must first specify what we mean by interactions and how they are estimated in real communities. Measuring species interactions is often difficult and prone to high uncertainty [26–29], and most empirical settings only give us access to averaged properties. In particular, the total effect of interactions on one species i by all other species can be inferred from its *relative yield*,

$$\eta_i = B_i/K_i, \tag{1}$$

the ratio of its abundance B_i in a community to its maximum abundance K_i (known as carrying capacity) without competitors in the same environment [30]. In the following we assume that the abundances reach and stabilize around some fixed values (the system reaches equilibrium), as will be relevant to the data analyzed below. We interpret species with higher η as *successful* competitors, as they benefit more

in total (or suffer less) from their interactions with others. The simplest way to model these interactions is to assume a linear dependence between species' relative yields,

$$\eta_i = 1 - \sum_{j \neq i} \beta_{ij} \eta_j, \quad \text{for all } i, \quad (2)$$

where β_{ij} is the effect of species j on species i (which need not be symmetrical; i.e., it can differ from the effect of i on j). β_{ij} is positive if the relation is deleterious, and negative if beneficial. We expect that in communities dominated by competition most β_{ij} values will be positive, but some negative values are allowed. The relationship (2) has had some predictive success on data [31,32]. It can also be derived from the classic Lotka-Volterra competition model, where it holds between coexisting species at equilibrium; see Eq. (6). The neutral theory of biodiversity [33] assumes $\beta_{ij} = 1$, while the existence of a pairwise coexistence mechanism for species i and j entails $\beta_{ij} < 1$. Note that here we focus on interactions between coexisting species, while interactions with species outside the community might be much stronger [19].

B. Probabilistic approach and predictions

For many β_{ij} matrices the solution of Eq. (2) will result in some negative η_i ; in fact, the probability that all η_i are positive (a *feasible* solution [34,35]) is exponentially small in species number S . Observing the coexistence of S species thus conveys some information about their interactions, but not enough to fully determine them: the equations (2) impose S constraints, while there are $S(S-1)$ unknown interaction coefficients β_{ij} . Therefore, many different interaction networks (here, coefficients β_{ij}) can generate the same equilibrium abundances.

Even when individual interaction coefficients are noisy, communitywide statistics, such as the expected strength of competition $\bar{\beta}$, can reliably be deduced from the species' relative yields [36] (see the Appendix D).

We therefore adopt a probabilistic approach (Fig. 2), and ask what is the *most likely* community structure, i.e., the set of features most widely shared among the many possible solutions. We first define a prior distribution on the matrix elements $P(\beta)$ that can be adapted to our biological knowledge of a given community. For the experiments below, we simply assume that each coefficient β_{ij} is drawn independently from a normal distribution with mean $\bar{\beta}$. We then compute how this prior is modified once restricted to networks that admit the equilibrium η_i .

To compute $P(\beta|\vec{\eta})$, we impose the S equilibrium conditions (2); i.e., we condition the prior distribution $P(\beta)$ to be in the hyperplane where $\sum_j \beta_{ij} \eta_j = 1$ for all i . This conditioning of a multivariate Gaussian distribution is still Gaussian, but with different statistics. This posterior distribution $P(\beta|\vec{\eta})$ is a new normal distribution over $S(S-1)$ -dimensional vectors β_{ij} , entirely specified by

its vector of means $E[\beta_{ij}|\vec{\eta}]$ and the correlation matrix $\text{corr}(\beta_{ij}, \beta_{ik}|\vec{\eta})$; see Fig. 3. Computing a posterior distribution given a prior and linear constraints (2) is a well-established problem in probability theory [37,38]. The derivation is given in Appendix A.

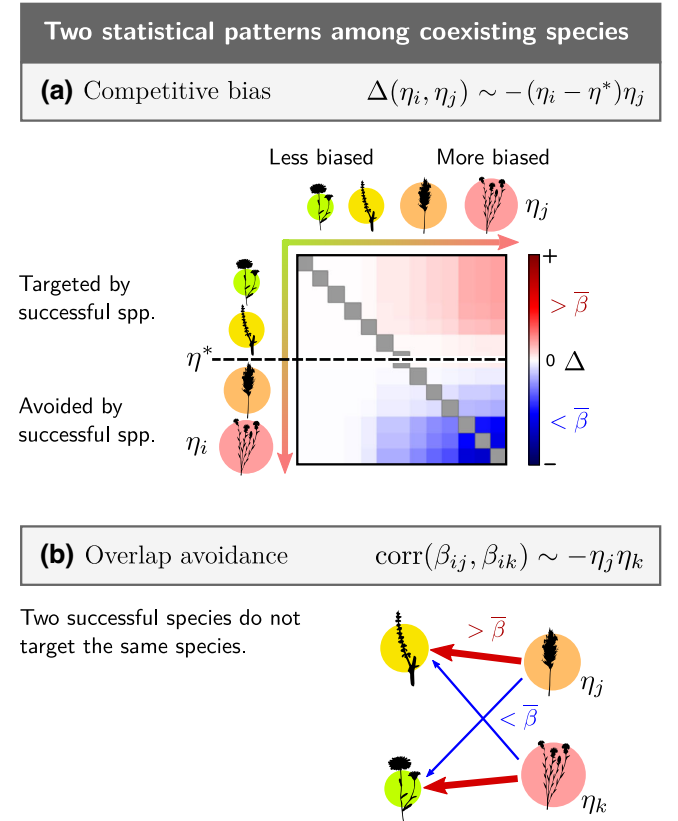


FIG. 3. The diffuse clique structure is characterized by two statistical patterns in how successful species compete. Any typical interaction network drawn from the posterior distribution $P(\beta|\vec{\eta})$ (see Fig. 2) will have similar statistical features. (a) Trend in the expectation $E[\beta_{ij}|\vec{\eta}]$ of competition strength Eq. (4). If all species competed with equal strength $\bar{\beta}$, we would expect any given species i to achieve the relative yield $\eta_i = \eta^*$ [Eq. (3)]. Given how much η_i differs from this baseline, we can infer how interactions most likely deviate from $\bar{\beta}$. We show this deviation $\Delta(\eta_i, \eta_j)$ for simulated data, in matrix form: each element shows the bias in the interaction effect of species j (column) on species i (row). Left to right: An unsuccessful species (low η_j) competes indiscriminately against others (white, $\Delta = 0$), whereas a successful species (high η_j) is a biased competitor. Top to bottom: Species with $\eta_i < \eta^*$ experience stronger competition from successful species (red, $\Delta > 0$), whereas species with $\eta_i > \eta^*$ experience weaker competition from them (blue, $\Delta < 0$). Together, these biases indicate the existence of a “clique” of species that compete less against each other, and more against all others, thus achieving higher relative yield than the baseline η^* . (b) Correlation structure (5) between columns of the interaction matrix: the effects of two successful species are anticorrelated, less likely to target the same species, whereas competition from unsuccessful species is indiscriminate.

We find that interactions β_{ij} should follow a statistical pattern characterized by two conditions, one on expectations and one on correlations, that both admit intuitive interpretations (Fig. 3). First, competition must be biased to explain which species are successful or not. Here, it is instructive to measure success relative to a baseline,

$$\eta^* = \frac{1 - \bar{\beta} \sum_i \eta_i}{1 - \bar{\beta}}, \quad (3)$$

which is the relative yield that a species *would* achieve if all interaction strengths were equal to the prior mean (i.e., if hypothetically $\beta_{ij} = \bar{\beta}$). When $\eta_i > \eta^*$, we therefore expect that species *i* suffers less competition than the prior mean, and conversely if $\eta_i < \eta^*$. In our calculation, this appears in the conditional expectation of the effect of *j* on *i* knowing their relative yields,

$$E[\beta_{ij} | \eta_i, \eta_j] = \bar{\beta} + (1 - \bar{\beta}) \Delta(\eta_i, \eta_j), \quad (4)$$

which deviates from the prior mean $\bar{\beta}$ by a *competitive bias*:

$$\Delta(\eta_i, \eta_j) = - \frac{(\eta_i - \eta^*) \eta_j}{\sum_{m, (m \neq i)} \eta_m^2}.$$

We see that this bias is not evenly distributed among species. Competition coming from unsuccessful species (low η_j) can be random without compromising the equilibrium. On the other hand, a species that is successful (high η_j) is likely to compete less on average against other

successful species, and to experience weaker competition from them [Fig. 3(a)].

The correlation coefficients also differ from the prior, in that successful species *j* and *k* are less likely to compete against the same target *i* [Fig. 3(b)]:

$$\text{corr}(\beta_{ij}, \beta_{ik} | \eta_i, \eta_j, \eta_k) = - \frac{\eta_j \eta_k}{\sum_{m, (m \neq i)} \eta_m^2}. \quad (5)$$

While the first pattern (4) determines the *expected* success of each species, the second pattern guarantees that each relative yield is *exactly* set to η_i . To show that, one can take the mean and variance of the rhs of Eq. (2), $1 - \sum_{j \neq i} \beta_{ij} \eta_j$, over the distribution $P(\boldsymbol{\beta} | \bar{\boldsymbol{\eta}})$. Using Eqs. (4) and (5), this is equal to η_i with zero variance. This result is expected by the definition of the conditioned $P(\boldsymbol{\beta} | \bar{\boldsymbol{\eta}})$, yet it reveals the role of the negative correlations, Eq. (5). Without it, deviations would likely drive some low- η species to extinction in a more random community.

Equations (4) and (5) are valid for any number of species *S*. For large *S*, the denominators $\sum_{m, (m \neq i)} \eta_m^2 \approx \sum_m \eta_m^2$ for all pairs to within $O(1/S)$, by adding the η_i^2 term. Then, Eq. (4) is simply bilinear in η_i, η_j , and Eq. (5) is bilinear in η_j, η_k .

So far, we have only used the fact that the community is at a fixed point with certain abundances. In Sec. III we touch on the stability of the state of the system, and how it might have formed.

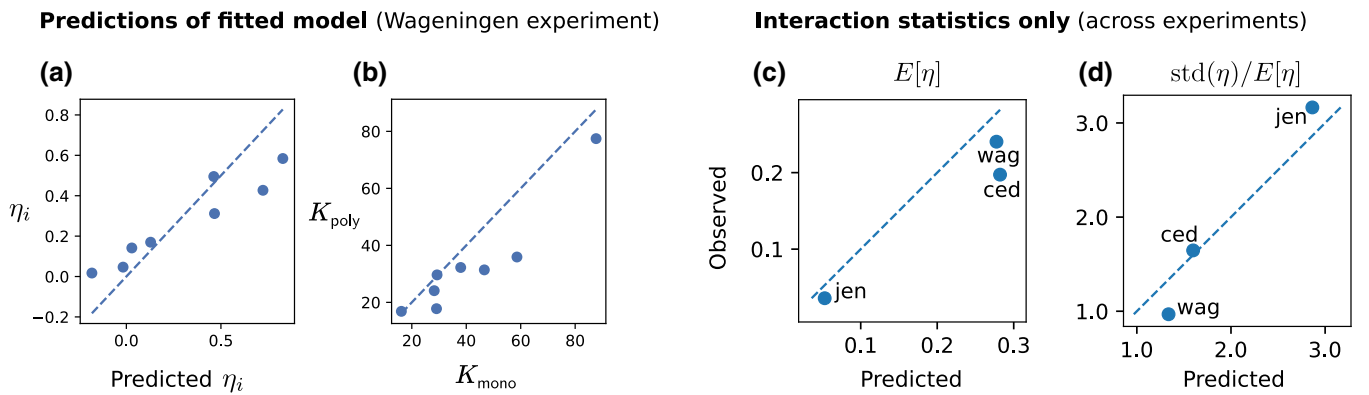


FIG. 4. Validation of the Lotka-Volterra model. The consistency of the equilibrium description (2) was validated through a series of tests. For the Wageningen grassland experiment (with $S = 8$ species), we find accurate predictions for the full fitted Lotka-Volterra model (dashed lines show a 1:1 relationship between prediction and measurement). (a) We compare the equilibrium values of $\eta_i = B_i/K_i$ in the full-diversity plot ($S = 8$) to the prediction $\eta_i = 1 - \sum_j \beta_{ij} \eta_j$, where interactions β_{ij} were inferred from all partial compositions (plots with $S < 8$). (b) Carrying capacities K_i inferred as the intercept of the multilinear regression from polyculture plots ($S > 1$) agree with direct measurements in monocultures ($S = 1$). (c),(d) Even when species are too numerous to allow a precise inference of all pairwise interactions, we can predict statistics of η_i using only the mean and variance of interactions β_{ij} in tested species pairs, following the methodology in Ref. [23]. Across the Wageningen, Cedar Creek Big Bio (16 species), and Jena (60 species) experiments, we find good agreement in predicted versus measured values for the mean in (c) and coefficient of variation in (d) of relative yields in the full-diversity plots.

C. Empirical validation

We now present an empirical validation of these patterns on experimental data in Figs. 5 and 6. We first searched for data that provide the equilibrium abundances of a set of coexisting species, as well as direct experimental measurements of the strength of pairwise interactions between these species. Our theory, parametrized only by species' relative yields in the full community, predicts statistical features of their interaction network, which we can compare to estimates of the same statistics in the measured interactions.

Grassland biodiversity experiments [39–41] provide an ideal test bed for inferring species interactions and mechanisms of coexistence. Each experiment contains a large number of plots delineated in a natural open environment, in which plant species are assembled in varying numbers and combinations, out of a pool of $S = 8$ –16 species depending on the experiment (see detailed description in the Supplemental Material [24]). Biomass in monoculture

(single-species plots) provides an estimate of the species' carrying capacities K_i .

Of these experiments, we focus in the main text on the Wageningen grassland experiment [39] for which almost all pairwise species combinations were realized, and which allows for precise testing of the equilibrium model. The experiment used $S = 8$ species, which grow naturally in that region. They are planted in 102 plots including all single-species plots, 24 out of 28 two-species plots, various four-species combinations, and the mixture of all 8 species. No treatment such as water or fertilization was applied, except for weeding out species that should not grow in each plot. Biomass was collected and measured annually over 12 years.

We first demonstrate the applicability of the equilibrium Lotka-Volterra model in Fig. 4. In the Wageningen grassland experiment especially, we observe a clear trend over time toward an equilibrium, namely a state in which species'

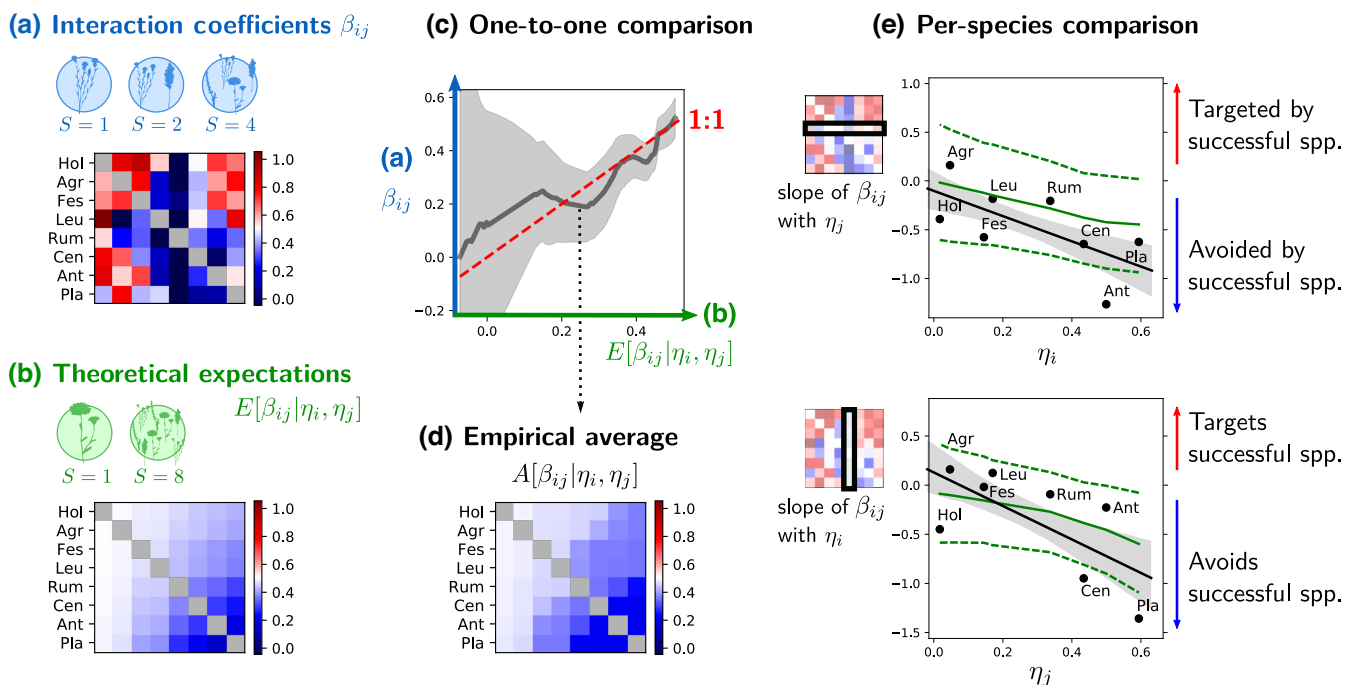


FIG. 5. Diffuse structure in the Wageningen grassland experiment. (a) Using many species combinations (56 sets of $S < 8$ species), we can fit interaction coefficients β_{ij} in Eq. (2) by multilinear regression and compute their mean $E[\beta] \approx 0.4$. (b) Using the relative yields η_i in the full community ($S = 8$ species), we predict the theoretical pattern of expectations (4) for each interaction [Fig. 3(a); here we see only negative biases in blue, indicating that all interactions are less competitive than the prior mean $\bar{\beta}$]. Abbreviations for species names are given in Sec. IV. (c)–(e) In our diffuse pattern, individual coefficients are expected to exhibit a large spread around their expectation $E[\beta_{ij}|\eta_i, \eta_j]$, and must be binned to compute empirical statistics. (c) We group coefficients β_{ij} by their associated η_i, η_j to compute the running average $A[\beta_{ij}|\eta_i, \eta_j]$ (gray curve, ± 1 standard deviation in shaded area). Its proximity to the dashed 1:1 line is one of multiple metrics of theory-data agreement. (d) We show the empirical running average $A[\beta_{ij}|\eta_i, \eta_j]$ in matrix form (median value for each species pair i, j), to be compared with the theoretical prediction $E[\beta_{ij}|\eta_i, \eta_j]$ in (b). This is a particular way of smoothing the empirical matrix β_{ij} shown in (a); see Sec. IV. (e) In another test of the theory, we group coefficients by species, i.e., either by row or by column in the matrix β_{ij} . We then compute how coefficients in row i (column j) vary with η_j (η_i). Each solid point is the linear regression slope within a row or column. The empirical values and their spread around the trend are both in good agreement with our theoretical predictions (mean trend in solid line, spread in dashed lines, ± 1 SD). The linear slope of the points matches quantitatively the theoretical trend in the mean, which is approximately linear as expected for large S .

abundances fluctuate around fixed values (see Fig. S2 in the Supplemental Material [24]). The Wageningen grassland experiment both displays the least noise in inferred coefficients, with the most extensive set of pair competition experiments ($\sim 85\%$ of all possible pairs), and replicates of the single-species and eight-species plots. The accuracy of biomass estimates over the years and over replicate plots is of comparable size, giving further confidence to the results.

The interactions were calculated using the multilinear fit of interactions [28] from plots with 1–4 species; see more details in Sec. IV.

Pairwise interactions almost all satisfy $\beta_{ij} < 1$, meaning that most species can coexist in pairs, with $E[\beta] \approx 0.4$ and $\text{std}(\beta) \approx 0.2$ showing a strong departure from the neutral hypothesis ($\beta_{ij} = 1$). Furthermore, these interactions β_{ij} , inferred only from plots with 1–4 species, correctly predict relative yields in the full eight-species community [Fig. 4(a)]. Thus, the biodiversity in this experiment is well explained by a simple equilibrium condition with pairwise interactions, without resorting to more complex explanations such as nonequilibrium coexistence [6] or higher-order interactions [42]. Following the method in Ref. [23], we show in Figs. 4(c) and 4(d) that even in high-diversity experiments where all pairwise interactions cannot be inferred precisely their statistics alone correctly predict the mean and variance of equilibrium relative yields.

Our theory then predicts statistical trends in species interactions, given their relative yields in the full community plots [43], with no adjustable parameters. We compare the fitted empirical interaction matrix to theoretically predicted expectations (4) and correlations (5).

We show in Fig. 5 the interaction matrix computed in the Wageningen grassland experiment [39], which supports our theory: individual coefficients β_{ij} display a random-looking spread, as we expect for a high-dimensional structure; yet we can group these coefficients in various ways to compute statistics, all of which concur with our predictions.

As the predicted probability distribution of interaction strengths resides in a high-dimensional space, various statistics can be formed to test its validity. We choose tests with two aims in mind. First, as the theory is probabilistic, all quantities are predicted to have a variation, so we choose quantities that are narrowly distributed. This allows us to compare predictions even when only one realization is given, provided S is large enough (a self-averaging quantity). For example, while the value of an individual matrix element is not expected to be strongly constrained, averages or slopes along rows or columns are more narrowly distributed. Second, we look for statistical tests that relate to the intuitive interpretation described above and summarized in Fig. 3.

As a first test, we bin interactions by their species' relative yields. We can then compute the empirical running average $A[\beta_{ij}|\eta_i, \eta_j]$, namely the average of β_{ij} for all species pairs i, j whose relative yields η_i and η_j give a similar predicted mean for β_{ij} , Eq. (4). This average is close

to a one-to-one relationship with the theoretical expectation $E[\beta_{ij}|\eta_i, \eta_j]$ [Fig. 5(c)].

In a second test, we group the coefficients by species: our theory (Fig. 3) predicts how the competition exerted and experienced by each species varies with the relative yields of competitors. Figure 5(e) shows that empirical statistics agree with both predictions, with a spread around the trend comparable to what we expect theoretically for eight species. These have a clear interpretation: for example, the slopes along the columns, in the bottom panel of Fig. 5(e),

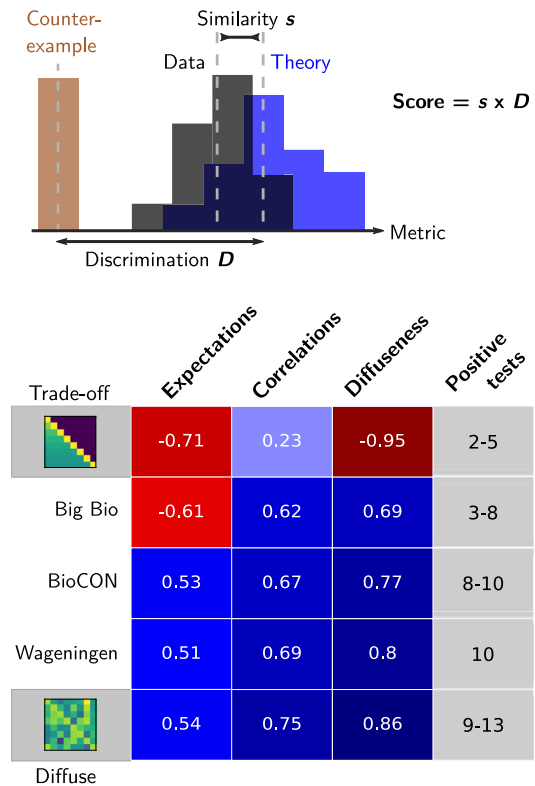


FIG. 6. Cross-experiment validation of the diffuse clique structure. Multiple quantitative tests are needed to confirm agreement between data and theoretical predictions while ruling out counterexamples. Therefore, we compute a series of metrics (defined in the Supplemental Material [24]) of agreement for conditional expectations $E[\beta_{ij}|\eta_i, \eta_j]$, correlations $\text{corr}(\beta_{ij}, \beta_{ik}|\eta_i, \eta_j, \eta_k)$, and diffuseness (whether interactions appear random). The first two metrics test the pattern shown in Fig. 3. We do not show each metric directly, because its predicted range is specific to each experiment. Instead, we assign a similarity score $s = +1$ if predicted and observed values differ by less than 2 standard deviations, -1 if they differ by more. We also compute a discrimination score D between 0 and 1 measuring how well the metric differentiates between our theory and a counterexample (see Sec. IV). The product $s \times D$ is shown here. Other metrics were also tested, and the last column reports the number (or range across treatments or simulation runs) of positive results out of all 13 tests shown in the Supplemental Material [24]. The first and last row display simulated communities that constitute either counterexamples (low-dimensional trade-off patterns) or examples of our theory.

correspond to the pattern presented in Fig. 3(a), according to which more successful species (higher η) compete less strongly with other successful species. As predicted, the data show a trend toward greater bias (more negative slope) as η grows. Moreover, the slope of these data points quantitatively matches the theoretically predicted slope. (The prediction is nearly a straight line at large S .) Finally, we compare the spread in the points around the slope of this line. This is done by generating matrices from the theoretical distribution, Eqs. (4) and (5), and measuring the spread of points. We see that the spread of measured points is consistent with the predicted one.

Turning to the correlations, Eq. (5) predicts that the effect of different species on the same target species will be negatively correlated [overlap avoidance, Fig. 3(b)]. We indeed find such negative correlations in the data. The average negative correlation is -0.086 ± 0.020 , significantly negative. This is to be compared with the prediction, -0.093 ± 0.002 .

This agreement between theory and data is precisely quantified for multiple experiments in Fig. 6. Our tests are designed to show that the empirical interactions appear too random to arise from a low-dimensional structure, yet exhibit the predicted pattern of means and correlations. We employ multiple metrics, each focusing on a different feature of our predictions, and we estimate how well each metric can discriminate between a positive example (a matrix generated according to our theory) and a negative one (here, a low-dimensional competition-colonization trade-off structure which does not follow our theory; see Fig. 2). Out of 13 tests detailed in the Supplemental Material [24], we show three representative examples: two evaluate the predictions in Fig. 3 and one quantifies the diffuse (random-looking) character of the interactions. These tests taken together indicate moderate to good agreement for the Big Bio, BioCON, and Wageningen experiments. The Wageningen grassland experiment displays both the least noise in inferred coefficients and the most consistent and precise match to theory.

III. DISCUSSION

We have identified the most parsimonious way in which a complex network of ecological interactions can be organized so that all species coexist. We have shown that this pattern indeed occurs in plant interactions measured in several biodiversity experiments. This invites a new, more collective outlook on how to explain and predict species coexistence and biodiversity.

Our theory predicts that, when complex interactions arise from many different factors, ecological communities will most generally display a fuzzy “clique” of competitors that are both successful and less likely to compete strongly with each other, surrounded by unsuccessful species with random-looking interactions. This picture differs in multiple respects from classic explanations of coexistence. By imposing only the weakest possible constraints upon the

many degrees of freedom in β_{ij} , it allows individual interactions to take almost arbitrary values. It does not suppose a measurable segregation of species into distinct niches. It also represents a form of collective organization, where coexistence arises, not from particular species traits, but from statistical biases distributed over all interactions. Accordingly, this structure becomes increasingly likely to occur (although increasingly diffuse and subtle) in more diverse communities.

Our results provide a test of how *typical* an empirical or synthetic interaction network is, given the observed abundances, i.e., how similar or different it is to the majority of networks admitting the same equilibrium $\vec{\eta}$. For instance, specific mechanisms such as the colonization-competition trade-off can give rise to communities that display different and even opposite correlations to our predictions (Fig. 6). Correspondingly, these interaction networks are quite distinctive, and tend to have low likelihood from a random prior. In empirical networks, finding such trends opposite to diffuse partitioning could be interpreted as evidence for some underlying biological processes imposing more structure than the minimum necessary for coexistence.

The probability distribution defined by Eqs. (4) and (5) allows us to make deterministic (self-averaging) predictions on the interaction network. This has advantages over direct tests for randomness, which are both conceptually and practically difficult, especially in the presence of noise due to measurement errors.

We stress that our results constitute a very stringent test for a theory of ecological coexistence. The fact that our simple multilinear model (2) correctly predicts coexistence (and even abundances) in various compositions is already a nontrivial result [28,29,31,32,36]. It suggests that more complex explanations, such as coexistence supported by dynamics [6] or higher-order interactions [42], are not required to explain the maintenance of biodiversity in these experiments. We go significantly further by demonstrating that the fitted interactions follow a theoretically predicted pattern, fully determined by measurements without any adjustable parameter. We have shown that our test can tell this pattern apart from a low-dimensional trade-off mechanism [44]. To reduce inference biases, we use distinct abundance data to parameterize our theory and to infer the empirical interactions. We rule out these relationships being artifacts of our method, showing them to be violated in sparse and noisy data or counterexamples to our theory; see Fig. 6. Consequently, we believe that the experimental evidence is not merely suggestive, but strongly supportive of our claim.

A. Why is the diffuse coexistence pattern likely?

We gave a probabilistic interpretation of diffuse partitioning. Naively, one might assume that coexistence requires all competitive interactions to be much weaker than in random assemblages of noncoexisting species. But finding a set of nothing but weak competitors is unlikely if

migration allows others to enter the community, and to account for that we impose some expected mean interaction strength. Instead, the most likely and parsimonious outcome is the differentiation of species into successful and less successful species, where the former are both more discriminate in their competition. Rather than have all species deviate strongly from the global distribution, this deviation is thus borne mostly by some species, in a way that ensures their success. This concentrates the nonrandom constraints into a fraction of important species, while allowing maximal random variation around this structure.

B. Dynamical considerations: Assembly and stability

Interestingly, the pattern obtained here is precisely the one obtained by an *assembly process* [25], where species migrate from a pool of S_{pool} species, and a subset of them forms a stably coexisting community. When the community follows Lotka-Volterra dynamics,

$$\frac{d\eta_i}{dt} = r_i \eta_i \left(1 - \eta_i - \sum_{j, (j \neq i)} \beta_{ij}^{\text{pool}} \eta_j \right) + \omega, \quad (6)$$

where ω represents small but positive migration, a fixed point of the dynamics will satisfy Eq. (2) for the S surviving species (those with $\eta_i > 0$ even when $\omega \rightarrow 0^+$). When the interactions between all species in the pool follow our prior distribution, the means and variances of the interactions between surviving species exactly follow the probability distribution in Eqs. (4) and (5). We interpret this to mean that, while ecological assembly must create some structure in the community, it deviates as little from the random prior as necessary to allow coexistence. This minimal structure is precisely the one that we would expect from our probabilistic argument above, applied to the S surviving species. Therefore, it appears that ecological assembly does not generate extraneous motifs (“spandrels” [45]) in the process of selecting species that persist together.

The derivation we put forward in this work is more phenomenological and less mechanical in nature. It explains how the pattern might apply to an experiment such as the Wageningen grassland experiment [39], where no species have gone extinct in the eight-species culture, but where other factors may have contributed to coexistence, considering that the species grow naturally in the same area which could entail prior assembly or coevolution, similarity in functional groups, etc.

Stability.—A fixed point of Eq. (6) must also be stable under small perturbations to the surviving species. In principle, the stability may differ for different matrices sampled from the same probability distribution for β , yet for large S typical matrices are either all stable or all unstable when $\text{var}(\beta_{ij})$ scales as $1/S$, with a sharp transition in terms of the system parameters [11,16,20]. In the case of interactions generated by assembly, it has been shown that the stability of the resulting network is not

affected by the pattern; namely, the matrices with the pattern are stable if and only if a matrix sampled from the fully random prior is stable [16,22,25].

If one allows *any* assignment of abundances $\vec{\eta}$ (not restricted to the outcomes of assembly), the situation is more complicated. There might not even exist a stable matrix β that admits these abundances as a stable fixed point. For example, for $S = 2$ and $\eta_1 = \eta_2 < 1/2$, the unique solution is $\beta_{12} = \beta_{21} = 1/\eta - 1$, which is unstable. Yet we prove in Appendix B that for large S with the same asymptotic scaling $\text{var}(\beta_{ij}) \sim 1/S$, and under additional weak conditions on $\vec{\eta}$, the conclusion from assembly scenario holds: the additional pattern does not affect stability, with samples of the posterior and prior probability distributions either both stable or both unstable.

In summary, we have introduced a novel way of thinking about species coexistence: not focusing on individual mechanisms, but predicting the universal statistical features that arise from combining many different coexistence mechanisms. We have quantitatively evidenced these features in real ecological communities. They reveal how *generic* an interaction network is: how statistically similar it is to most possible networks admitting the same equilibrium (Fig. 2). These features are not a necessary consequence of equilibrium coexistence: they can be violated in some communities, and these departures can hint at other biologically important low-dimensional mechanisms, such as simple trade-offs between ecological traits [44]. Instead, these features suggest the existence of a collective, intrinsically high-dimensional community organization. In such ecosystems, coexistence cannot be understood by analyzing particular species traits or environmental factors.

While our examples center on diffuse competition (dense interactions between many competitors), the underlying theoretical findings can be extended to any interaction network, be it noncompetitive, sparse, or qualitative. The formulas given above have been derived assuming that interactions are close to being fully random, but the same reasoning can be adapted to other priors on network structure. This can allow future extensions to other ecological networks such as food webs, and to generative processes such as speciation, which introduce distinct nonrandom, yet nonfunctional, patterns (spandrels) into interaction networks [45].

The classic alternative to niche theory has been the neutral theory of biodiversity [33], a null model that posits identical species without coexistence mechanisms. That model is empirically invalid here, as we observe heterogeneous and moderate species interactions that often allow pairwise coexistence. By contrast, our theory proposes a null model for complex communities with a large variety of coexistence mechanisms. Our results imply the existence of a spectrum of possibilities between classic trait-based theories and complex network approaches and provide a conclusive empirical test of collective organization in many-species coexistence.

IV. MATERIALS AND METHODS

A. Experimental data and interactions

We employ data from four grassland biodiversity experiments in Wageningen, Netherlands [39], Cedar Creek, MN, (the Big Biodiversity [41] and BioCON [40] experiments), and Jena [46]. Each experiment uses a pool of species seeded or planted in various combinations, including some or all possible monocultures ($S = 1$ species), some partial compositions, and all species planted together. We removed the first two years for all experiments, as they showed clear evidence of transient dynamics (Supplemental Material [24], Sec. C). The species pool in the Wageningen biodiversity experiment comprises four grass species (*Agrostis capillaris* L., *Anthoxanthum odoratum* L., *Festuca rubra* L., *Holcus lanatus* L.) and four dicot species (*Centaurea jacea* L., *Leucanthemum vulgare* Lamk., *Plantago lanceolata* L., *Rumex acetosa* L.).

For each experiment, we first split monoculture ($S = 1$) data in two distinct sets, to be used separately, and computed the species' carrying capacities K_i within each set. The first set of monocultures and all plots with $1 < S < S_{\max}$ (where S_{\max} is the experiment's maximal plot diversity) were used to infer the interaction matrix β_{ij} using the hyperplane (multilinear) least-squares fit proposed by Xiao *et al.* [28] (see Appendix C). The second set of monocultures and the species abundance B_i in plots with $S = S_{\max}$ were then used to compute the relative yields $\eta_i = B_i/K_i$ in the full community. All calculations were performed 250 times, using different bootstrapped sample means as values for K_i and B_i . Each calculation led to a different set of η_i , β_{ij} , and β (see Appendixes C and D for calculation details). Error bars were also estimated from the bootstrapping procedure.

The multilinear fit of interactions [28] provided robust estimates of the effect of abundant species, but random fluctuations of η_i between plots could lead to very large (and highly variable) inferred per-capita effects for rare species with small η_j . To avoid this issue, we first removed all species that had a reported abundance of 0 more than 90% of the time in plots where they had been planted, then removed coefficients β_{ij} whose variance between bootstrapped replicas was larger than the variance between coefficients in the matrix. This procedure retained all coefficients in the Wageningen experiment, but only around 60% of coefficients in the other experiments. Given that the Wageningen experiment gave more robust interaction values, we used it to assess our hypothesis that observed abundances are primarily determined by fixed pairwise species interactions according to Eq. (2). Figure 4 shows strong empirical support for the hypothesis in this experiment. Interaction estimates from other experiments were less robust and might be affected by nonlinearity, transient dynamics, stochasticity, and errors (Supplemental Material [24], Sec. D). The Jena experiment has the largest pool of $S = 60$ species and therefore a very small fraction of duocultures are represented. As a

consequence, we only use it for a simple check of statistical predictions with the Lotka-Volterra model (Fig. 4).

B. Validation of theoretical predictions

We tested the two components of the diffuse clique pattern. Starting with the pattern of means, Eq. (4), we must compare the measured values of β_{ij} (hereafter y) to their theoretical expectation $E[\beta_{ij}|\eta_i, \eta_j]$ (hereafter x). To obtain an empirical estimate of the expectation for a single interaction coefficient, we performed a running average: for each point (x, y) , we replaced its y coordinate by the average \bar{y} within a window centered on x and spanning 10% of the x axis; we also measure the 90% confidence interval over bootstrapped values [Fig. 5(c)]. We then grouped all values \bar{y} associated with the same species pair (i, j) , took their median, and reconstructed an empirical matrix of expectations B_{ij} [shown in Fig. 5(d)]. We also grouped coefficients by species i or j and performed regressions against η_j or η_i , respectively [Fig. 5(e)], as well as the bilinear regression of β_{ij} against $\eta_i\eta_j$ (the score computed from this metric is shown in Fig. 6, first column).

We proceeded similarly to test the pattern of correlations, Eq. (5). Defining $d_{ij} = \beta_{ij} - E[\beta_{ij}|\eta_i, \eta_j]$ and the identity matrix \mathbb{I} , we computed for each species triplet (i, j, k) the value $y = \mathbb{I}_{jk} - d_{ij}d_{ik}/\text{mean}(d^2)$, where the denominator is the sample mean over all pairs. We then did a regression of y against the prediction $x = -\eta_j\eta_k/\sum_{l \neq i} \eta_l^2$ (Fig. 6, second column).

The diffuse nature of our pattern means that we expect the interaction matrix β_{ij} to appear almost random. True randomness is notoriously difficult to demonstrate [47], so we focused here on a more intuitive property: smoothness. The low-dimensional trade-off that we use as a counterexample creates a smoothly varying matrix β_{ij} , whereas our diffuse pattern cannot. As a simple metric of smoothness, we measured differences between adjacent coefficients and computed the fraction of these differences that are smaller than $\text{std } \beta/2$ (Fig. 6, third column).

For each of these metrics, we computed the distribution of values obtained from bootstrapped empirical matrices and found its mean and variance $\mu_{\text{expt}}, \sigma_{\text{expt}}^2$. We also computed the distribution of values in matrices generated according to our theory ($\mu_{\text{theor}}, \sigma_{\text{theor}}^2$), and in matrices generated with a competition-colonization trade-off ($\mu_{\text{cc}}, \sigma_{\text{cc}}^2$), with the same equilibrium as the data (see Appendix B for details). In Fig. 6, we define similarity as

$$s = \begin{cases} 1 & \text{if } |\mu_{\text{expt}} - \mu_{\text{theor}}| < 2\sigma_{\text{theor}} \\ -1 & \text{otherwise,} \end{cases} \quad (7)$$

which states in a simple binary score whether observed values fall within the confidence interval (2 standard deviations) of predicted values. We define discrimination as

$$D = \left[1 + \min \left(\frac{|\mu_{\text{expt}} - \mu_{\text{theor}}|}{\sigma_{\text{expt}} + \sigma_{\text{theor}}}, \frac{|\mu_{\text{cc}} - \mu_{\text{theor}}|}{\sigma_{\text{cc}} + \sigma_{\text{theor}}} \right)^{-1} \right]^{-1}, \quad (8)$$

which quantifies how well a given metric can differentiate between patterns (D goes to 0 when standard deviations are significantly larger than the interval between means). The product $s \times D$ gives the scores shown in Fig. 6.

This study brought together existing data that were obtained upon request (Wageningen biodiversity experiment data from Van Ruijven and Berendse [39]) and data that are publicly available [48–50]. Data represented in Figs. 5 and 6 are available in Ref. [51].

ACKNOWLEDGMENTS

We thank J.-F. Arnoldi, F. Isbell, and Y. Zelnik for comments. Our gratitude goes to J. van Ruijven for sharing data from the Wageningen grassland experiment. M. B., C. d. M., and M. L. were supported by the TULIP Laboratory of Excellence (ANR-10-LABX-41) and by the BIOTASES Advanced Grant, funded by the European Research Council under the European Union’s Horizon 2020 research and innovation programme (666971). G. B. was supported by the Israel Science Foundation (ISF) Grant No. 773/18. Experimental work at Cedar Creek was supported by grants from the U.S. National Science Foundation Long-Term Ecological Research Program (LTER) including DEB-0620652 and DEB-1234162, and further support was provided by the Cedar Creek Ecosystem Science Reserve and the University of Minnesota.

APPENDIX A: DERIVATION OF THE PATTERN

In this Appendix, Eqs. (4) and (5) are derived. In the prior probability distribution, the coefficients in the matrix β for $i \neq j$ are independent, identically distributed (i.i.d) Gaussian random variables with mean $\bar{\beta} \equiv \langle \beta_{ij} \rangle$ and variance $\langle \beta^2 \rangle_c \equiv \langle \beta_{ij}^2 \rangle_c$. It is conditioned on

$$\sum_{j, (j \neq i)} \beta_{ij} \eta_j + \eta_i = 1,$$

for every i . Consider $\vec{\beta}_i$, the i th row without β_{ii} (it has $S - 1$ elements). The probability distribution depends on η_i and the vector of abundances without η_i , denoted $\vec{\eta}_{\setminus i}$, and given by

$$P(\vec{\beta}_i | \vec{\eta}) \propto \text{normal}(\vec{\beta}_i; \langle \beta^2 \rangle_c \mathbf{I}, \vec{\mu} = \bar{\beta} \vec{u}) \times \delta(\vec{\beta}_i \cdot \vec{\eta}_{\setminus i} - (1 - \eta_i)),$$

where \vec{u} is the column vector $\vec{u} = (1, 1, \dots, 1)^T$, $\delta(\dots)$ is the Dirac δ function, and we do not make explicit the normalization factor as it does not depend on the β_{ij} variables. We would like to write this as a Gaussian probability distribution without a δ function. Instead, it will have a rank-deficient correlation matrix \mathbf{C} .

To proceed, consider an orthonormal change of basis:

$$\vec{x} = \mathbf{R} \vec{\beta}_i.$$

We choose the first row of \mathbf{R} to be $\vec{a} \equiv \vec{\eta}_{\setminus i} / |\vec{\eta}_{\setminus i}|$, and the rest of the rows are chosen orthogonal to it and normalized (e.g., via a Gram-Schmidt process). Thus, $\mathbf{R} \vec{\eta}_{\setminus i} = |\vec{\eta}_{\setminus i}| \vec{w}$, with $\vec{w} \equiv (1, 0, \dots, 0)^T$. In the rotated space,

$$\vec{\beta}_i \cdot \vec{\eta}_{\setminus i} = (\mathbf{R} \vec{\beta}_i) \cdot (\mathbf{R} \vec{\eta}_{\setminus i}) = |\vec{\eta}_{\setminus i}| \vec{x} \cdot \vec{w} = |\vec{\eta}_{\setminus i}| x_1.$$

Therefore, the distribution of \vec{x} is

$$P(\vec{x}) = \text{normal}(\vec{x}; \langle \beta^2 \rangle_c \mathbf{I}, \mathbf{R} \bar{\beta} \vec{u}) \delta(|\vec{\eta}_{\setminus i}| x_1 - (1 - \eta_i)).$$

We can readily rewrite this as a Gaussian distribution without the δ function, since it represents S independent random variables with a constraint only on the first one. The loss of variance in the first dimension means that the correlation matrix becomes

$$\mathbf{C}_x = \langle \beta^2 \rangle_c \mathbf{I} - \langle \beta^2 \rangle_c \begin{pmatrix} 1 & & & \\ & 0 & & \\ & & 0 & \\ & & & \ddots \end{pmatrix}.$$

While in the means vector $\vec{\mu}_x$, we have $\langle x_1 \rangle = (1 - \eta_i) / |\vec{\eta}_{\setminus i}|$, and the rest are unchanged,

$$\vec{\mu}_x = \left[\mathbf{I} - \begin{pmatrix} 1 & & & \\ & 0 & & \\ & & 0 & \\ & & & \ddots \end{pmatrix} \right] \mathbf{R} \bar{\beta} \vec{u} + \vec{w} (1 - \eta_i) / |\vec{\eta}_{\setminus i}|.$$

Together,

$$P(\vec{x}) = \text{normal}(\vec{x}; \mathbf{C}_x, \vec{\mu}_x).$$

Rotating back to $\vec{\beta}_i = \mathbf{R}^{-1} \vec{x} = \mathbf{R}^T \vec{x}$, we find

$$P(\vec{\beta}_i | \vec{\eta}_{\setminus i}) = \text{normal}(\vec{\beta}_i; \mathbf{C}_{\vec{\beta}_i}, \vec{\mu}_{\vec{\beta}_i}),$$

with

$$\begin{aligned} \mathbf{C}_{\bar{\beta}_i} &= \mathbf{R}^T \mathbf{C}_x \mathbf{R} = \langle \beta^2 \rangle_c [\mathbf{I} - \bar{a} \bar{a}^T] = \langle \beta^2 \rangle_c \left[\mathbf{I} - \frac{\bar{\eta}_{\setminus i} \bar{\eta}_{\setminus i}^T}{|\bar{\eta}_{\setminus i}|^2} \right], \\ \bar{\mu}_{\bar{\beta}_i} &= \mathbf{R}^T \left\{ \left[\mathbf{I} - \begin{pmatrix} 1 & & & \\ & 0 & & \\ & & \ddots & \\ & & & 0 \end{pmatrix} \right] \mathbf{R} \bar{\beta} \bar{u} + \bar{w} \frac{(1 - \eta_i)}{|\bar{\eta}_{\setminus i}|} \right\} \\ &= [\mathbf{I} - \bar{a} \bar{a}^T] \bar{\beta} \bar{u} + \bar{a} \frac{(1 - \eta_i)}{|\bar{\eta}_{\setminus i}|} \\ &= \bar{\beta} \left[\bar{u} - \frac{\bar{\eta}_{\setminus i} \bar{\eta}_{\setminus i}^T}{|\bar{\eta}_{\setminus i}|^2} \bar{u} \right] + \frac{(1 - \eta_i)}{|\bar{\eta}_{\setminus i}|^2} \bar{\eta}_{\setminus i}. \end{aligned}$$

Written elementwise, they read

$$\begin{aligned} \mathbf{C}_{\bar{\beta}_i}(k, l) &= \langle \beta^2 \rangle_c \left[\delta_{k,l} - \frac{\eta_k \eta_l}{\sum_{j, (j \neq i)} \eta_j^2} \right], \\ \bar{\mu}_{\bar{\beta}_i}(k) &= \bar{\beta} - \bar{\beta} \frac{\eta_k \sum_{l, (l \neq i)} \eta_l}{\sum_{j, (j \neq i)} \eta_j^2} + \frac{(1 - \eta_i)}{\sum_{j, (j \neq i)} \eta_j^2} \eta_k \\ &= \bar{\beta} + \frac{1 - \eta_i - \bar{\beta} \sum_{l, (l \neq i)} \eta_l}{\sum_{j, (j \neq i)} \eta_j^2} \eta_k \\ &= \bar{\beta} - \frac{1}{\sum_{j, (j \neq i)} \eta_j^2} \eta_i \eta_k + \frac{1 - \bar{\beta} \sum_{j, (j \neq i)} \eta_j}{\sum_{j, (j \neq i)} \eta_j^2} \eta_k, \end{aligned}$$

which are precisely Eqs. (4) and (5). The correlations can be interpreted as a projector that prevents fluctuations in the $\sum_j \beta_{ij} \eta_j$ direction.

The derivation can be turned into an algorithm: the matrix \mathbf{R} can be generated and \bar{x} can be easily sampled, as implemented in R in the code that we provide in the link [51] in the main text.

APPENDIX B: STABILITY

Here we look at the stability of dynamical Lotka-Volterra equations, Eq. (6), for matrices β sampled from the conditioned distribution defined by Eqs. (4) and (5), compared with matrices sampled from the prior distribution (i.i.d. variables). We show, under certain conditions at large S , that β sampled with the pattern is stable if and only if a β sampled from the prior would be. This means that the pattern neither stabilizes nor destabilizes the dynamical system. This same conclusion was reached for communities assembled dynamically [16,20,22,25]; the difference being that there $\bar{\eta}$ are also determined by the assembly process, while here it is given as an input.

We look at the spectrum of β . The system is stable if and only if for all eigenvalues λ the real part is positive, $\text{Re}(\lambda) > 0$ [52]. To study stability at the large S limit we need to define the scaling in that limit. Generally, the stability depends on $\text{std}(\beta_{ij})$ through the rescaled

variable $\sigma \equiv \sqrt{S} \text{std}(\beta_{ij})$ [11,16,20]. A sharp transition is therefore obtained for large S with the scaling $\text{std}(\beta_{ij}) = \sigma/\sqrt{S}$.

Numerical tests show that the pattern of correlations, Eq. (5), does not seem to affect the distribution of eigenvalues. We therefore focus on the effect of the biases of the means Eq. (4).

The argument below assumes that no η_i is much larger than the others, i.e., $\eta_i^2 / \sum_k \eta_k^2 \rightarrow 0$ for large S . Secondly, it requires that at large S , the biases in the means, Eq. (4), are individually small compared to the self-regulation, $\beta_{ii} = 1$. This does not mean that the pattern is not required for coexistence: without it many species would go extinct [20]. Nor does it need to be small compared to the off-diagonal elements β_{ij} . For Eq. (4) to be small compared to one, it is sufficient that $\bar{\beta} \rightarrow 0$ as $S \rightarrow \infty$, e.g., $\bar{\beta} \sim S^{-g}$. To see this, note that from Eq. (2), $\eta_i = 1 - \sum_{j \neq i} \beta_{ij} \eta_j$, we find that $\eta_i \sim 1/(S\bar{\beta})$, so $1/(S\eta_i) \rightarrow 0$ as $S \rightarrow \infty$. If $\bar{\beta} \leq O(1/S)$, then $\eta_i = O(1)$ from the ‘‘disordered’’ contribution with $\text{std}(\beta_{ij}) = \sigma/\sqrt{S}$. In both cases, Eq. (4) is $O(S^{-g})$.

We show that with these assumptions, the conditioning of β with Eq. (4) does not change the stability of the system, namely the sign of $\min_\lambda \text{Re}(\lambda)$.

An *unconditioned* matrix β_{uncond} can be written as

$$\beta_{\text{uncond}} = (1 - \bar{\beta}) \mathbf{I} + \bar{\beta} u^T u + \sigma \mathbf{A}$$

where \mathbf{I} is the identity matrix, u a column vector $u = (1, 1, \dots)$, and \mathbf{A} a random matrix with i.i.d random variables with $\text{var}(A_{ij}) = 1/S$ and zero mean. According to the circular law [53], the eigenvalues of \mathbf{A} are uniformly distributed in the circle $|\lambda| < 1$. The term $\bar{\beta} u^T u$ has a single nonzero eigenvalue $\bar{\beta} S$, and so acts as a low-rank perturbation on \mathbf{A} . This is known [54] to change the spectrum by merely adding an eigenvalue at $\bar{\beta} S$. Finally, the scaled identity term $(1 - \bar{\beta}) \mathbf{I}$ shifts the spectrum by $\lambda \rightarrow \lambda + 1 - \bar{\beta}$. All together, the matrix β_{uncond} is stable when $\sigma/(1 - \bar{\beta}) < 1$.

For the conditioned matrix β_{cond} , Eq. (4) shifts the means with

$$\beta^{\text{cond}} = (1 - \bar{\beta}) \mathbf{I} + \mathbf{G}^{\text{cond}} + \sigma \mathbf{A},$$

where the matrix \mathbf{G}^{cond} (already for large S)

$$G_{ij}^{\text{cond}} = \bar{\beta} + \frac{1 - (1 - \bar{\beta}) \eta_i - \bar{\beta} \sum_k \eta_k}{\sum_{k, (k \neq i)} \eta_k^2} \eta_j.$$

The second term $[1 - (1 - \bar{\beta}) \eta_i - \bar{\beta} \sum_{k, (k \neq i)} \eta_k^2] \eta_j$ should not appear on the diagonal. It is here that we use the assumption above, and note that on the diagonal we get $1 + O(S^{-g})$, so adding it also to the diagonal will have a negligible effect on the spectrum (essentially, the shifting that \mathbf{I} creates will be corrected by small fluctuating

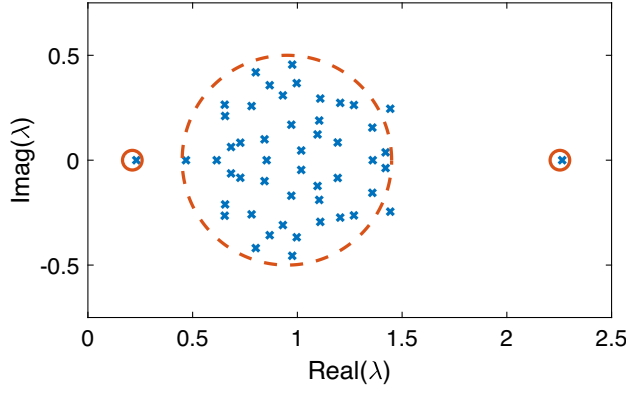


FIG. 7. Spectrum of conditioned β . Crosses: eigenvalues of a matrix β conditioned with the pattern defined by Eqs. (4) and (5), with $S = 50$. Dashed line: circle within which β^{cond} should have eigenvalues due to $\sigma\mathbf{A}$. Small circles: predicted positions of additional two eigenvalues. Other parameters: $\eta_{1\dots 10} = 3, \eta_{11\dots 50}$ are i.i.d variables, uniformly sampled in $[0, 1.5]$; $\bar{\beta} = 0.05$; $\sigma = 0.5$.

Secondly, we use the assumption that $\eta_i^2 / \sum_k \eta_k^2 \rightarrow 0$ to add η_i^2 to the denominator. Thus, we obtain

$$G_{ij}^{\text{cond}} = \bar{\beta} + \frac{1 - (1 - \bar{\beta})\eta_i - \bar{\beta}I_1}{I_2}\eta_j,$$

where $I_k \equiv \sum_i \eta_i^k$, also for the diagonal.

By the lemma below, the matrix \mathbf{G}^{cond} is of rank 2, and its nonzero eigenvalues satisfy $\lambda_{1,2} \geq -(1 - \bar{\beta})$. This means that \mathbf{G}^{cond} is a low-rank perturbation of $\sigma\mathbf{A}$. If the unconditioned system is stable $\sigma/(1 - \bar{\beta}) < 1$, then the $\text{Re}(\lambda) > -(1 - \bar{\beta})$ for all eigenvalues of $\sigma\mathbf{A}$, and therefore also of $\mathbf{G}^{\text{cond}} + \sigma\mathbf{A}$. After the shift due to $(1 - \bar{\beta})\mathbf{I}$, all eigenvalues of β^{cond} have positive real parts. Figure 7 shows an example of a spectrum of a sampled matrix, compared with this theory.

Lemma.— \mathbf{G}^{cond} has rank 2, and the nonzero eigenvalues satisfy $\lambda_{1,2} \geq -(1 - \bar{\beta})$.

Proof.—We look at the eigenvalues of \mathbf{G}^{cond} . Let $\vec{u} \equiv (1, 1, 1, \dots)$. For a vector \vec{v} ,

$$\sum_j G_{ij} v_j = \bar{\beta}(\vec{u} \cdot \vec{v}) + \frac{1 - (1 - \bar{\beta})\eta_i - \bar{\beta}I_1}{I_2}(\vec{\eta} \cdot \vec{v}).$$

Therefore any vector for which $\vec{u} \cdot \vec{v} = 0 = \vec{\eta} \cdot \vec{v}$ is an eigenvector with zero eigenvalue. This is a subspace of dimension $S - 2$. The remaining subspace is spanned by $\vec{u}, \vec{\eta}$. Indeed,

$$\begin{aligned} \mathbf{G}^{\text{cond}}\vec{\eta} &= F_{11}\vec{\eta} + F_{12}\vec{u}, \\ \mathbf{G}^{\text{cond}}\vec{u} &= F_{21}\vec{\eta} + F_{22}\vec{u}, \end{aligned}$$

with

$$\mathbf{F} = \begin{bmatrix} -(1 - \bar{\beta}) & 1 \\ -(1 - \bar{\beta})\frac{I_1}{I_2} & \bar{\beta}S + (1 - \bar{\beta})\frac{I_1}{I_2} \end{bmatrix},$$

and $\lambda_{1,2}$ are the eigenvalues of \mathbf{F} . To show that $\lambda_{1,2} \geq -(1 - \bar{\beta})$, we show that the matrix $\mathbf{F} + (1 - \bar{\beta})\mathbf{I}$ has two positive eigenvalues. This follows from

$$\det[\mathbf{F} + (1 - \bar{\beta})\mathbf{I}] = (1 - \bar{\beta})\frac{I_1}{I_2} > 0$$

and

$$\text{Tr}[\mathbf{F} + (1 - \bar{\beta})\mathbf{I}] = \bar{\beta}\left(S - \frac{I_1^2}{I_2} - 1\right) + \frac{I_1}{I_2} + 1 \geq \frac{I_1}{I_2} + 1 - \bar{\beta} > 0,$$

where we used the fact that $I_1^2/I_2 = S[(S^{-1}\sum_i \eta_i^2)/(S^{-1}\sum_i \eta_i)^2]^{-1} \leq S$. ■

APPENDIX C: FITTING AND TESTING THE EQUILIBRIUM MODEL

This Appendix describes how the data are fitted to an equilibrium model and the interactions β_{ij} are deduced.

Given the biomasses $N_i^{(1)}$ in monocultures and $N_i^{(w)}$ in other plots with composition w , we define the relative yield:

$$\eta_i^{(w)} = N_i^{(w)}/N_i^{(1)}. \quad (\text{C1})$$

We should use a single such value per composition, since we will take it to represent the true equilibrium relative yield of that species in that composition. The simplest way to then deduce interactions is directly from the relative yields in duocultures [compositions w with $S(w) = 2$ species]:

$$\beta_{ij} = \frac{1 - \eta_i^{(w)}}{\eta_j^{(w)}}. \quad (\text{C2})$$

In practice, using only duoculture relative yields leads to rather noisy results, and it discards useful information contained in more diverse plots.

Following Xiao *et al.* [28] we instead infer the interaction matrix β_{ij} as follows. Provided that species i is not extinct, all equilibria containing that species are predicted (under Lotka-Volterra assumptions) to verify

$$0 = 1 - \eta_i^{(w)} - \sum_{j \neq i} \beta_{ij} \eta_j^{(w)}. \quad (\text{C3})$$

Under the prior assumption that all β_{ij} are independent, we can infer the vector β_{ij} for each species i independently. It is then a simple case of multilinear regression, minimizing the sum of squares over all compositions w :

$$\min_{\beta_{ij}} \left[\sum_w \left(1 - \eta_i^{(w)} - \sum_{j \neq i} \beta_{ij} \eta_j^{(w)} \right)^2 \right]. \quad (\text{C4})$$

In the case of the Wageningen grassland experiment, for each species i , there are seven parameters β_{ij} and at most 30 plots in which the species is present with significant abundance. For other experiments, there are fewer different compositions per species, meaning that there is a larger risk of overfitting some interactions; in some, there are pairs of species that never occur in the same composition, hence their interactions are left blank and ignored thereafter.

When we then test this model and our theoretical predictions on the equilibrium state of the most diverse plots, we use interactions β_{ij} fitted using all compositions except the most diverse [$S(w) < S_{\max}$]. To make sure that the data used for fitting and for testing are entirely distinct, we even split monocultures into those used for computing relative yields $\eta_i^{(w)}$ in the most diverse plots and those used to compute it in all the other plots.

The same process can be applied directly to species biomasses,

$$0 = K_i - N_i^{(w)} - \sum_{j \neq i} \beta_{ij} N_j^{(w)}, \quad (\text{C5})$$

so as to infer the carrying capacity K_i , not from monocultures only, but as the intercept of the multilinear regression of N_i against other biomasses N_j (i.e., the asymptotic value of N_i in the absence of other species).

We perform two tests of the validity of the fitted linear model (Fig. 4): we use fitted interactions to predict the maximum-diversity equilibrium abundances, and we compare estimates of K_i from monocultures to those obtained as intercepts of the above regression from all plots except monocultures. These tests (and additional tests shown in the Supplemental Material [24]) are especially successful for the Wageningen experiment, which we therefore propose as a reference experiment for any further investigation based on Lotka-Volterra competition models.

APPENDIX D: ESTIMATING THE PRIOR PARAMETERS

There are two important steps in computing our new theoretical predictions: measuring the relative yields in the full community η_i and inferring the parameter $\bar{\beta}$ which enters into the pattern of means [Eq. (4)]. We now discuss the second step. This parameter can be interpreted as the mean of the prior distribution of interactions $P(\beta)$ before we constrain it to ensure coexistence. It is therefore different from $E[\beta]$, the expected value of all interactions measured among coexisting species (see Appendix D 1). For instance, in a community assembly experiment where some species go to extinction, $\bar{\beta}$ would be the average interaction strength between all species in the preassembly

pool and $E[\beta]$ the average interaction strength in the observed community of surviving species, which would typically be less competitive.

1. Getting pool parameters from interactions between coexisting species

Given the average interaction strength $E[\beta]$ between coexisting species, our theory makes it possible to compute the original interaction strength $\bar{\beta}$ in the pool of all possible species (i.e., in the prior). Let us rewrite the pattern of means [Eq. (4)] as

$$E[\beta_{ij} | \eta_i, \eta_j] = \bar{\beta} + \frac{\eta_j}{S \text{mean}(\eta^2) - \eta_i^2} \times [1 - (1 - \bar{\beta})\eta_i - \bar{\beta}S \text{mean}(\eta)], \quad (\text{D1})$$

given the mean $\bar{\beta}$ of the prior distribution $P(\beta)$. We will compare this pattern to fits and use it to generate matrices from the conditioned random ensemble. However, to do so, we must know $\bar{\beta}$.

By integrating over η_i and η_j , we see that the average in the matrix of coexisting species is displaced from the prior mean,

$$E[\beta_{ij}] = \bar{\beta} [1 + \text{mean}(\eta)Q_2 - S \text{mean}(\eta)^2 Q_1] + \text{mean}(\eta)(Q_1 - Q_2), \quad (\text{D2})$$

with

$$Q_1 = \text{mean} \left[\frac{1}{S \text{mean}(\eta^2) - \eta_i^2} \right],$$

$$Q_2 = \text{mean} \left[\frac{\eta_i}{S \text{mean}(\eta^2) - \eta_i^2} \right]. \quad (\text{D3})$$

As a consequence, by inverting Eq. (D2), we can infer $\bar{\beta}$ the mean in the prior distribution (or the preassembly pool of species) if we know the empirical average $E[\beta_{ij}]$ among coexisting species.

2. Mean field estimate

Getting a naive estimate of $\bar{\beta}$ is immediate, following a classic ‘‘mean field’’ approximation [36]: if all interactions are exactly $\beta_{ij} = \bar{\beta}$ [i.e., if our prior distribution $P(\beta)$ has zero variance], then all relative yields should be equal and given by

$$\eta_i = \bar{\eta} = \frac{1}{1 + (S - 1)\bar{\beta}}. \quad (\text{D4})$$

We can invert this formula to obtain $\bar{\beta}$, but for heterogeneous relative yields, this parameter is strongly underestimated when compared to other methods (and also when compared to its true value in simulations). For a better (but

still rough) approximation, we use the observed average relative yield mean η_i to estimate the *realized* interaction strength:

$$E[\beta_{ij}]_{\text{naive}} = \frac{1}{S} \left[\frac{1}{\text{mean}(\eta_i)} - 1 \right]. \quad (\text{D5})$$

From this, we can estimate $\bar{\beta}_{\text{naive}}$ by inverting Eq. (D2) as described in the previous section.

This estimate gives similar but slightly worse results than those shown in the main text, because it often underestimates the average strength of competition in a heterogeneous community. Note that if all species survive, we can also have a rough estimate of the variance of β [23]:

$$\text{var}(\beta)_{\text{naive}} = \frac{1}{S} \left[1 - \frac{\text{mean}(\eta)^2}{\text{mean}(\eta^2)} \right]. \quad (\text{D6})$$

3. Estimating $E[\beta_{ij}]$

Results shown in the main text use the empirical mean $E[\beta_{ij}]$ directly computed from the inferred interactions β_{ij} . This is the most direct option, but it requires knowledge of the interaction matrix, which is not available outside of special experimental setups such as those studied here. In other systems, we could attempt other ways of estimating the empirical mean. In particular, we can compute the *fixed point*: the value such that $E[\beta_{ij}] = \bar{\beta}$, meaning that adding the constraint of coexistence (or letting assembly run) will not change the average interaction. If we have no other information about the system, this is the most likely interaction strength given that we see these species coexist with observed relative yields η_i :

$$E[\beta_{ij}] = \bar{\beta} \Leftrightarrow \bar{\beta} = \frac{\text{mean}(\eta)(Q_1 - Q_2)}{\text{mean}(\eta)Q_2 - S \text{mean}(\eta)^2 Q_1}. \quad (\text{D7})$$

This is one of our methods for estimating $\bar{\beta}$ (two more are detailed in the Supplemental Material [24]) and it gives good results in simulations and in the Wageningen experiment, but predicts weaker competition than when computed directly from the matrix β_{ij} in the other experiments, suggesting that species in these experiments may already represent a pre-selected subset of a larger, more competitive pool.

We also note that the correlation pattern,

$$\text{cov}(\beta_{ij}, \beta_{ik}) = \sigma_{\beta}^2 \left[\delta_{jk} - \frac{\eta_j \eta_k}{S \text{mean}(\eta^2) - \eta_i^2} \right], \quad (\text{D8})$$

given the variance σ_{β}^2 of the prior distribution indicates that

$$\text{var}(\beta) = \sigma_{\beta}^2 [1 - \text{mean}(\eta^2)Q_1], \quad (\text{D9})$$

which we can invert to obtain σ_{β} from a realized matrix.

-
- [1] G. F. Gause, *The Struggle for Existence* (Williams and Wilkins, Baltimore, 1934).
 - [2] D. Tilman, *Resource Competition and Community Structure* (Princeton University Press, Princeton, NJ, 1982).
 - [3] D. Tilman, *Diversification, Biotic Interchange, and the Universal Trade-Off Hypothesis*, *Am. Nat.* **178**, 355 (2011).
 - [4] R. MacArthur, *Species Packing, and What Competition Minimizes*, *Proc. Natl. Acad. Sci. U.S.A.* **64**, 1369 (1969).
 - [5] S. A. Levin, *Community Equilibria and Stability, and an Extension of the Competitive Exclusion Principle*, *Am. Nat.* **104**, 413 (1970).
 - [6] P. Chesson, *Quantifying and Testing Coexistence Mechanisms Arising from Recruitment Fluctuations*, *Theor. Popul. Biol.* **64**, 345 (2003).
 - [7] G. Barabás, *Rafael D'Andrea, and Simon Maccracken Stump, Chesson's Coexistence Theory*, *Ecol. Monogr.* **88**, 277 (2018).
 - [8] S. Saavedra, R. P. Rohr, J. Bascompte, O. Godoy, N. J. B. Kraft, and J. M. Levine, *A Structural Approach for Understanding Multispecies Coexistence*, *Ecol. Monogr.* **87**, 470 (2017).
 - [9] R. Levins and D. Culver, *Regional Coexistence of Species and Competition between Rare Species*, *Proc. Natl. Acad. Sci. U.S.A.* **68**, 1246 (1971).
 - [10] D. Tilman, *Competition and Biodiversity in Spatially Structured Habitats*, *Ecology* **75**, 2 (1994).
 - [11] R. M. May, *Will a Large Complex System be Stable?*, *Nature (London)* **238**, 413 (1972).
 - [12] E. P. Wigner, *On the Distribution of the Roots of Certain Symmetric Matrices*, *Ann. Math.* **67**, 325 (1958).
 - [13] P. W. Anderson, *Absence of Diffusion in Certain Random Lattices*, *Phys. Rev.* **109**, 1492 (1958).
 - [14] M. Mezard and A. Montanari, *Information, Physics, and Computation* (Oxford University Press, New York, 2009).
 - [15] D. J. Amit, H. Gutfreund, and H. Sompolinsky, *Spin-Glass Models of Neural Networks*, *Phys. Rev. A* **32**, 1007 (1985).
 - [16] M. Opper and S. Diederich, *Phase Transition and 1/f Noise in a Game Dynamical Model*, *Phys. Rev. Lett.* **69**, 1616 (1992).
 - [17] C. K. Fisher and P. Mehta, *The Transition between the Niche and Neutral Regimes in Ecology*, *Proc. Natl. Acad. Sci. U.S.A.* **111**, 13111 (2014).
 - [18] D. A. Kessler and N. M. Shnerb, *Generalized Model of Island Biodiversity*, *Phys. Rev. E* **91**, 042705 (2015).
 - [19] Y. Fried, D. A. Kessler, and N. M. Shnerb, *Communities as Cliques*, *Sci. Rep.* **6**, 35648 (2016).
 - [20] G. Bunin, *Ecological Communities with Lotka-Volterra Dynamics*, *Phys. Rev. E* **95**, 042414 (2017).
 - [21] M. Tikhonov and R. Monasson, *Collective Phase in Resource Competition in a Highly Diverse Ecosystem*, *Phys. Rev. Lett.* **118**, 048103 (2017).

- [22] G. Biroli, G. Bunin, and C. Cammarota, *Marginally Stable Equilibria in Critical Ecosystems*, *New J. Phys.* **20**, 083051 (2018).
- [23] M. Barbier, J.-F. Arnoldi, G. Bunin, and M. Loreau, *Generic Assembly Patterns in Complex Ecological Communities*, *Proc. Natl. Acad. Sci. U.S.A.* **115**, 2156 (2018).
- [24] See Supplemental Material at <http://link.aps.org/supplemental/10.1103/PhysRevX.11.011009> for details on data preprocessing, additional tests, and a list of experiments.
- [25] G. Bunin, *Interaction Patterns and Diversity in Assembled Ecological Communities*, [arXiv:1607.04734](https://arxiv.org/abs/1607.04734).
- [26] C. Mazancourt, F. Isbell, A. Larocque, F. Berendse, E. Luca, J. B. Grace, B. Haegeman, H. W. Polley, C. Roscher, B. Schmid *et al.*, *Predicting Ecosystem Stability from Community Composition and Biodiversity*, *Ecol. Lett.* **16**, 617 (2013).
- [27] C. K. Fisher and P. Mehta, *Identifying Keystone Species in the Human Gut Microbiome from Metagenomic Timeseries Using Sparse Linear Regression*, *PLoS One* **9**, e102451 (2014).
- [28] Y. Xiao, M. T. Angulo, J. Friedman, M. K. Waldor, S. T. Weiss, and Y.-Yu. Liu, *Mapping the Ecological Networks of Microbial Communities*, *Nat. Commun.* **8**, 2042 (2017).
- [29] J. Friedman, L. M. Higgins, and J. Gore, *Community Structure Follows Simple Assembly Rules in Microbial Microcosms*, *Nat. Ecol. Evol.* **1**, 0109 (2017).
- [30] M. Loreau, *From Populations to Ecosystems: Theoretical Foundations for a New Ecological Synthesis (MPB-46)* (Princeton University Press, Princeton, NJ, 2010).
- [31] D. S. Maynard, J. T. Wootton, C. A. Serván, and S. Allesina, *Reconciling Empirical Interactions and Species Coexistence*, *Ecol. Lett.* **22**, 1028 (2019).
- [32] D. S. Maynard, Z. R. Miller, and S. Allesina, *Predicting Coexistence in Experimental Ecological Communities*, *Nat. Ecol. Evol.* **4**, 91 (2020).
- [33] S. P. Hubbell, *The Unified Neutral Theory of Species Abundance and Diversity* (Princeton University Press, Princeton, NJ, 2001).
- [34] A. Roberts, *The Stability of a Feasible Random Ecosystem*, *Nature (London)* **251**, 607 (1974).
- [35] M. Dougoud, L. Vinckenbosch, R. P. Rohr, L.-F. Bersier, and C. Mazza, *The Feasibility of Equilibria in Large Ecosystems: A Primary but Neglected Concept in the Complexity-Stability Debate*, *PLoS Comput. Biol.* **14**, e1005988 (2018).
- [36] H. Fort, *Quantitative Predictions from Competition Theory with an Incomplete Knowledge of Model Parameters Tested against Experiments across Diverse Taxa*, *Ecol. Model.* **368**, 104 (2018).
- [37] E. T. Jaynes, *On the Rationale of Maximum-Entropy Methods*, *Proc. IEEE* **70**, 939 (1982).
- [38] F. Vrins, *Sampling the Multivariate Standard Normal Distribution under a Weighted Sum Constraint*, *Risks* **6**, 64 (2018).
- [39] J. Van Ruijven and F. Berendse, *Long-Term Persistence of a Positive Plant Diversity–Productivity Relationship in the Absence of Legumes*, *Oikos* **118**, 101 (2009).
- [40] P. B. Reich, D. Tilman, S. Naeem, D. S. Ellsworth, J. Knops, J. Craine, D. Wedin, and J. Trost, *Species and Functional Group Diversity Independently Influence Biomass Accumulation and Its Response to CO₂ and N*, *Proc. Natl. Acad. Sci. U.S.A.* **101**, 10101 (2004).
- [41] D. Tilman, P. B. Reich, and J. M. H. Knops, *Biodiversity and Ecosystem Stability in a Decade-Long Grassland Experiment*, *Nature (London)* **441**, 629 (2006).
- [42] M. M. Mayfield and D. B. Stouffer, *Higher-Order Interactions Capture Unexplained Complexity in Diverse Communities*, *Nat. Ecol. Evol.* **1**, 0062 (2017).
- [43] As shown in the equations above, our theoretical predictions also depend on our prior for the mean interaction strength $\bar{\beta}$. But this quantity is determined by the empirical average $E[\beta]$ (see Appendix D). Hence, our theory has no freely adjustable parameter.
- [44] A. T. Clark, C. Lehman, and D. Tilman, *Identifying Mechanisms That Structure Ecological Communities by Snapping Model Parameters to Empirically Observed Tradeoffs*, *Ecol. Lett.* **21**, 494 (2018).
- [45] S. Valverde, J. Piñero, B. Corominas-Murtra, J. Montoya, L. Joppa, and R. Solé, *The Architecture of Mutualistic Networks as an Evolutionary Spandrel*, *Nat. Ecol. Evol.* **2**, 94 (2018).
- [46] A. Weigelt, E. Marquard, V. M. Temperton, C. Roscher, C. Scherber, P. N. Mwangi, S. Felten, N. Buchmann, B. Schmid, E.-D. Schulze *et al.*, *The Jena Experiment: Six Years of Data from a Grassland Biodiversity Experiment*, *Ecology* **91**, 930 (2010).
- [47] M. Lachmann, M. E. J. Newman, and C. Moore, *The Physical Limits of Communication or Why Any Sufficiently Advanced Technology Is Indistinguishable from Noise*, *Am. J. Phys.* **72**, 1290 (2004).
- [48] Big Bio, <http://www.cedarcreek.umn.edu/research/data>.
- [49] BioCON, <http://www.biocon.umn.edu/>.
- [50] Jena, <http://jenaexperiment.iee.uni-jena.de/>.
- [51] <https://github.com/mrcbarbier/diffuseclique>.
- [52] This is stability under a perturbation to the carrying capacities. The stability under small excursions of the abundances has been found to coincide with it in previous works [16,20,22], and here in additional numerics.
- [53] T. Tao, V. Vu, and M. Krishnapur, *Random Matrices: Universality of ESDs and the Circular Law*, *Ann. Probab.* **38**, 2023 (2010).
- [54] T. Tao, *Outliers in the Spectrum of iid Matrices with Bounded Rank Perturbations*, *Probab. Theory Relat. Fields* **155**, 231 (2013).